RESEARCH ARTICLE
doi: 10.2306/scienceasia1513-1874.2025.095

ScienceAsia 51 (6): 2025: ID 2025095: **1–11**

Dynamics of a fractional order delayed predator-prey system with ratio-dependence

Xiao Tang[a,b], **Ahmadjan Muhammadhaji**[a,b,*]

[a] College of Mathematics and System Sciences, Xinjiang University, Urumqi 83, China
[b] The Key Laboratory of Applied Mathematics of Xinjiang Uygur Autonomous Region, Xinjiang University, Urumqi 83, China

*Corresponding author, e-mail: ahmatjanam@aliyun.com

Received 12 May 2025, Accepted 21 Oct 2025
Available online 22 Dec 2025

ABSTRACT: In this study, we investigate the dynamical behavior of a fractional-order delayed predator-prey system with Holling-II type functional response modeled by fractional-order delay differential equations. Initially, the Laplace transform technique is employed to establish the boundedness of solutions in the absence of time delay. The existence of solutions is then rigorously established using the zero-point existence theorem, followed by an analysis of the local stability properties of equilibrium points. By treating the time delay as a bifurcation parameter, we derive explicit conditions for the occurrence of Hopf bifurcation, demonstrating that the system loses stability and generates a family of periodic oscillations as the delay parameter crosses critical threshold values. Finally, numerical simulations are conducted to validate the theoretical results: specific parameter configurations are selected, and different fractional orders alongside varying delay magnitudes are systematically explored to corroborate the analytical findings.

KEYWORDS: predator-prey system, Holling-II functional response, delay, fractional order, stability, Hopf burfication

MSC2020: 34K20 34A37 34K37

INTRODUCTION

The predator-prey relationship constitutes a foundational theme in ecology and applied mathematics, characterizing a fundamental ecological interaction marked by reciprocal dependence and constraint between species. This dynamic not only governs species survival and proliferation but also dictates the stability and evolutionary pathways of ecosystems. Through mathematical modeling, researchers rigorously analyze the dynamic equilibrium between these populations and the influences of diverse factors on this balance. The Lotka-Volterra (L-V) predator-prey model, initially formulated in the 1940s by ecologist Alfred Lotka [1] and mathematician Vito Volterra [2], formalizes trophic interactions, serving as a cornerstone for interspecific competition theory. Subsequent theoretical advancements include Yüzbaşı [3] investigation of discrete time-delay effects in L-V systems and Ma et al [4] analysis of predator intraspecific interference, illustrating the model's adaptability to complex ecological scenarios.

The classical L-V model, while foundational for describing ecosystem dynamics, is inherently constrained to pairwise species interactions, a simplification that starkly contrasts with the intricate multispecies interdependencies characteristic of natural ecological systems. Moreover, its reliance on integer-order differential equations proves inadequate for capturing critical biological phenomena-such as memory effects and hereditary traits-that manifest as historical state dependencies in population dynamics. To bridge this gap and enhance predictive accuracy, researchers have progressively refined mathematical methodologies, most notably through the integration of fractional calculus into predator-prey modeling frameworks.

Fractional derivatives, distinguished by their nonlocal properties, offer a robust framework for encoding memory effects, as they inherently incorporate the system's historical behavior via integral operators of non-integer order. This feature enables fractional-order models to more faithfully represent the historical dependence of population trajectories compared to their integer-order counterparts. Empirical implementations include Ma's [5] delayed reaction-diffusion model, which investigates competition between two predator species for a shared prey, and Bi et al [6] fractional-order system with cross-diffusion and herd behavior, designed to analyze three-dimensional pattern formation. Concurrently, higher-dimensional extensions-such as Das' [7] three-dimensional model exploring predator odor-mediated interactions, where competitor species are negatively impacted while prey populations benefit-have expanded the L-V paradigm to accommodate emergent ecological feedbacks. Subsequent studies [8–10] have further elaborated on these multi-dimensional frameworks, enhancing their capacity to reflect real-world complexity. The model's utility extends beyond ecology, finding applications in economics [11, 12], biomedical engineering [13], and social dynamics [14, 15], where its foundational principles inform the analysis of interdependent systems across disciplines.

A further limitation of the conventional L-V model

lies in its reliance on linear functional responses to characterize predation dynamics, a simplification that diverges from empirical observations of sophisticated nonlinear feeding behaviors in natural systems. Functional responses-defined as the relationship between prey density and individual predator consumption rates-are central to predator-prey modeling, with Holling-type formulations emerging as a standard framework for capturing nonlinearity. For example, Kumar et al [16] analyzed a system featuring coexisting predators with divergent responses: one exhibiting a linear functional form and the other a Holling-II response, revealing differential impacts on prey stability. Rihan [17] extended this to fractional-order delayed systems with Holling-III responses, incorporating infectious disease dynamics in predator populations, while Wang [18] explored Holling-IV formulations. Studies integrating Beddington-DeAngelis responses [19, 20] have demonstrated that functional response specificity profoundly influences system stability and oscillatory behavior.

Beyond response types, researchers have integrated additional ecological mechanisms—including prey refuges, harvesting practices, disease transmission, and fear effects [21–27]—into predator-prey models. These extensions not only enrich the theoretical landscape but also enhance the realism of mathematical representations, enabling more accurate simulations of natural systems. Collectively, such advancements address the classical L-V model's simplifications, fostering a more nuanced understanding of population dynamics that accounts for historical memory, multispecies interactions, and nonlinear trophic relationships.

Building on the foundational work of previous studies, this paper aims to investigate an enhanced three-dimensional fractional-order delayed predator-prey model derived from the L-V framework, where a Holling-II functional response is employed to characterize the trophic interaction between one predator and its prey. The model is motivated by a real-world ecological scenario in the Arctic tundra: lemmings-highly fecund rodent prey-support Arctic foxes, which exhibit a Holling-II functional response due to their specialized reliance on lemmings. Snowy owls, conversely, represent generalist predators with a broader diet and prey-switching behavior, introducing interspecific competition with Arctic foxes for shared lemming resources. This multi-species interaction exemplifies the model's capacity to capture complex ecological dynamics, rendering it an ideal candidate for examining the effects of time delays and fractional-order dynamics on population fluctuations, such as cyclic oscillations and outbreak patterns in lemming populations.

The main contributions of this paper are as follows: (1) For the first time, a delayed fractional-order predator-prey model incorporating two competing predators and a Holling-II functional response is established, with a focus on how fractional-order properties and time delay influence the systems dynamic behaviors. (2) The inclusion of competition between two predators (both preying on a single prey population) represents a distinctive feature of this study. This setup aligns closely with real-world ecological scenarios and offers a more precise portrayal of the complex dynamics exhibited by interacting species in nature. (3) A detailed Hopf bifurcation analysis of the proposed fractional-order delayed system is conducted, clarifying the conditions under which bifurcations occur. (4) By treating predator digestion delay as the bifurcation parameter, we investigate the effects of both this delay and the Holling-II functional response on the stability of the fractional-order system. This analytical approach enables the identification of rich dynamic behaviors of the system, providing key insights into its nonlinear dynamics.

THE MODEL AND PRELIMINARIES

In [28], the authors investigated the following L-V predator-prey model with time delays

$$\begin{aligned}
x_1'(t) &= x_1(t)\big[r_1(t)-a_{11}(t)x_1(t-\tau_{11}(t)) \\
&\quad -a_{12}(t)x_2(t-\tau_{12}(t))-a_{13}(t)x_3(t-\tau_{13}(t))\big], \\
x_2'(t) &= x_2(t)\big[-r_2(t)+a_{21}(t)x_1(t-\tau_{21}(t)) \\
&\quad -a_{22}(t)x_2(t-\tau_{22}(t))-a_{23}(t)x_3(t-\tau_{23}(t))\big], \\
x_3'(t) &= x_3(t)\big[-r_3(t)+a_{31}(t)x_1(t-\tau_{31}(t)) \\
&\quad -a_{32}(t)x_2(t-\tau_{32}(t))-a_{33}(t)x_3(t-\tau_{33}(t))\big],
\end{aligned}$$

where $x_1(t)$ represents the density of the prey species at time t, while $x_2(t)$ and $x_3(t)$ represent the densities of the predator species at time t. Leveraging Krasnoselskii's fixed-point theorem and constructing a Lyapunov function, the authors derived a set of readily verifiable sufficient conditions for the existence of solutions.

In [16], the authors investigated a Caputo fractal-fractional ecological model featuring one prey species $p(t)$ and two predator species $x(t)$ and $y(t)$, formulated as:

$$\begin{aligned}
{}^cD^q x(t) &= x(t)\left(\frac{a_1 p(t)}{1+bp(t)}-d_1\right), \\
{}^cD^q y(t) &= y(t)\left(a_2 p(t)-d_2\right), \\
{}^cD^q p(t) &= p(t)(1-p(t))-\frac{a_1 p(t)x(t)}{1+bp(t)}-a_2 p(t)y(t),
\end{aligned}$$

where $x(t)$ represents a nonlinear predator (characterized by a Holling-II-type functional response) and $y(t)$ denotes a linear predator (exhibiting a direct proportional feeding rate). The study focused on establishing the uniqueness and existence of solutions under fractional-order dynamics. Additionally, bifurcation diagrams and phase portraits were employed to numerically characterize the system's behavior, providing

Table 1 Biological meaning of the parameters in system (1).

Parameter	Biological Interpretation
α	Half-saturation constant for prey consumption by predator $y(t)$.
b_1	Intrinsic birth rate of the prey population.
b_2	Density-independent mortality rate for predator $y(t)$.
b_3	Density-independent mortality rate for predator $z(t)$.
a_{11}	Self-regulation coefficient (intraspecific competition) for the prey.
a_{12}	Searching efficiency or attack rate of predator $y(t)$ on the prey.
a_{13}	Searching efficiency or attack rate of predator $z(t)$ on the prey.
a_{21}	Conversion efficiency of prey biomass to offspring for predator $y(t)$.
a_{22}	Intraspecific competition coefficient among predator $y(t)$ individuals.
a_{23}	Competition coefficient between predators $y(t)$ and $z(t)$.
a_{31}	Conversion efficiency of prey biomass to offspring for predator $z(t)$.
a_{32}	Competition coefficient between predators $z(t)$ and $y(t)$.
a_{33}	Intraspecific competition coefficient among predator $z(t)$ individuals.
τ	Time delay representing predation lag or digestive processing time.

insights into its dynamical responses across parameter spaces.

In the interdisciplinary domains of dynamical systems and ecology, differential equations serve as indispensable tools for modeling population dynamics and interspecies interactions. By leveraging fractional-order calculus, these models offer a more precise representation of systems exhibiting memory effects and hereditary properties-features inherent in biological populations-while time delays explicitly account for the delayed impacts of trophic interactions, such as predation lag or reproductive timing mismatches. Over the past few decades, a substantial body of research has been dedicated to the dynamics of fractional-order dynamical models. For relevant studies, reference may be made to Refs. [29–35] and the references cited therein. In addition, in the current research on predator-prey systems, most existing achievements focus on single or dual-factor combinations such as "integer-order + ratio-dependence", "fractional-order + no delay", or "integer-order + delay" (for example, Ref. [28] only analyzes the stability of integer-order systems without ratio-dependence, and reference [16] only discusses the dynamic behavior of fractional-order predator systems without delay). However, the "dynamic analysis of systems coupling fractional-order, delay, and ratio-dependence" remains a direction to be breakthrough.

Building on prior research and theoretical advancements in fractional ecology, this paper integrates these three key factors (the "memory" characterized by fractional-order derivatives, the "lag effect of population interaction" reflected by delay, and the "nonlinear dependence of predators on prey density" embodied by ratio-dependence) into the same predator-prey model for the first time. This model is more in line with the actual scenario of "multi-factor joint action" in real ecological systems, forming a core system framework that is distinct from existing studies. Moreover, the time-delayed fractional-order predator-prey model proposed in this paper is constructed to capture the intricate interaction dynamics among three coexisting species. Thus, the proposed model is formulated as follows:

$$\begin{aligned}
{}^{c}D^{q}x(t) &= x(t)\Big(b_1 - a_{11}x(t) - \frac{a_{12}y(t)}{\alpha + x(t-\tau)} - a_{13}z(t)\Big),\\
{}^{c}D^{q}y(t) &= y(t)\Big(-b_2 + \frac{a_{21}x(t-\tau)}{\alpha + x(t-\tau)} - a_{22}y(t) - a_{23}z(t)\Big),\\
{}^{c}D^{q}z(t) &= z(t)\Big(-b_3 + a_{31}x(t) - a_{32}y(t) - a_{33}z(t)\Big),
\end{aligned} \tag{1}$$

with initial conditions:

$$x(0) > 0, \quad y(0) > 0, \quad z(0) > 0.$$

In system (1), $x(t)$ represents the population density of the prey species at time t, and $y(t)$ and $z(t)$ represent the population densities of two distinct predator species at time t. Specifically, we postulate that the predator $y(t)$ exhibits a non-linear predation behavior characterized by a Holling-II functional response. In contrast, the predator $z(t)$ demonstrates a linear predation pattern.

The following Table 1 is an academically refined version of the parameter table, adhering to formal scientific notation and terminology.

Now, we introduce the definition and fundamental properties of the Caputo derivative, concepts that will be invoked in subsequent analytical developments.

Definition 1 ([29]) The Caputo derivative is defined by:

$${}^{c}D^{q}f(t) = \frac{1}{\Gamma(m-q)}\int_0^t (t-s)^{m-q-1} f^{(m)}(s)\,\mathrm{d}s,$$

where $m-1 < \varphi < m$ for some $m \in \mathbb{N}$, and $\Gamma(\cdot)$ denotes the Gamma function, mathematically characterized as:

$$\Gamma(\alpha) = \int_0^\infty \mathrm{e}^{-\nu}\nu^{\alpha-1}\,\mathrm{d}\nu.$$

The Laplace transform of the Caputo fractional-order derivative is given by:

$$\mathscr{L}\{{}^cD^q f(t);s\} = s^q F(s) - \sum_{i=0}^{n-1} s^{q-i-1} f^{(i)}(0),$$

where $F(s) = \mathscr{L}\{f(t)\}$ represents the Laplace transform of $f(t)$. In the specific case where the initial derivatives satisfy $f^{(i)}(0) = 0$ for all $i = 0, 1, \ldots, n-1$, the transform simplifies to $\mathscr{L}\{{}^cD^q f(t)\}_s = s^q F(s)$.

Theorem 1 ([29]) *For any positive real numbers $c > 0$ and $d > 0$, and $K \in \mathbb{C}^{n\times n}$, the following Laplace transform relation holds:*

$$\mathscr{L}\left\{t^{d-1}E_{c,d}(Kt^c)\right\} = \frac{p^{c-d}}{p^c - K}, \quad \text{for } \mathrm{Re}(p) > \|K\|^{\frac{1}{c}},$$

where $\mathrm{Re}(p)$ denotes the real part of the complex number p, and $E_{c,d}$ represents the Mittag-Leffler function, which is defined as $E_{c,d}(z) = \sum_{n=0}^{\infty} \frac{z^n}{\Gamma(cn+d)}$.

Theorem 2 ([29]) *Let us consider the following fractional-order system:*

$${}^cD^q x(t) = f(x), \quad x(0) = x_0,$$

where $q \in (0,1)$ and $x \in \mathbb{R}^n$. The equilibrium points of this system are determined by the solutions of the equation $f(x) = 0$. An equilibrium point of the system is said to be locally asymptotically stable if, for the Jacobian matrix $J = \frac{\partial f}{\partial x}$ evaluated at this equilibrium point, all its eigenvalues λ_j satisfy the condition $\left|\arg(\lambda_j)\right| > \frac{q\pi}{2}$.

THE EXISTENCE, BOUNDEDNESS AND NON-NEGATIVITY OF THE SOLUTIONS

In this section, we investigate the properties of system (1) under the condition of $\tau = 0$. Firstly, we discuss the existence and uniqueness of solutions for the model (1). Relevant studies on the existence and uniqueness of solutions for delayed predator-prey models can be found in [36–38].

Theorem 3 *System (1) admits a unique solution for all non-negative initial conditions.*

Proof: In order to prove the theorem, we consider a region $\Psi \times (t_0, T)$, $T < \infty$, where $\Psi = \left\{(x,y,z) \in \mathbb{R}^3, |, \max(|x|,|y|,|z|) = M\right\}$. Then, we consider a map

$$F(X) = (F_1(X), F_2(X), F_3(X)),$$

where $X = (x,y,z)$ and $\widehat{X} = (\widehat{x}, \widehat{y}, \widehat{z})$,

$$\begin{aligned}
F_1(X) &= x(t)\left(b_1 - a_{11}x(t) - \tfrac{a_{12}y(t)}{\alpha + x(t-\tau)} - a_{13}z(t)\right),\\
F_2(X) &= y(t)\left(-b_2 + \tfrac{a_{21}x(t-\tau)}{\alpha + x(t-\tau)} - a_{22}y(t) - a_{23}z(t)\right),\\
F_3(X) &= z(t)(-b_3 + a_{31}x(t) - a_{32}y(t) - a_{33}z(t)).
\end{aligned}$$

For any $X, \widehat{X} \in \Psi$, we have

$$\begin{aligned}
&\|F(X) - F(\widehat{X})\| = \sum_{i=1}^{3} \left|F_i(X) - F_i(\widehat{X})\right|\\
&= \left|x\left(b_1 - a_{11}x - \tfrac{a_{12}y}{\alpha+x} - a_{13}z\right) - \left[\widehat{x}\left(b_1 - a_{11}\widehat{x} - \tfrac{a_{12}\widehat{y}}{\alpha+\widehat{x}} - a_{13}\widehat{z}\right)\right]\right|\\
&+ \left|y\left(-b_2 + \tfrac{a_{21}x}{\alpha+x} - a_{22}y - a_{23}z\right) - \left[\widehat{y}\left(-b_2 + \tfrac{a_{21}\widehat{x}}{\alpha+\widehat{x}} - a_{22}\widehat{y} - a_{23}\widehat{z}\right)\right]\right|\\
&+ |z(-b_3 + a_{31}x - a_{32}y - a_{33}z) - [\widehat{z}(-b_3 + a_{31}\widehat{x} - a_{32}\widehat{y} - a_{33}\widehat{z})]|\\
&\leqslant [b_1 + (a_{31} + 2a_{11} + a_{13})M + \frac{(a_{21}+a_{12})(M\alpha + M^2)}{\alpha^2}]|x - \widehat{x}|\\
&+ [b_2 + (a_{32} + 2a_{22} + a_{23})M + \frac{(a_{21}+a_{12})(M\alpha + M^2)}{\alpha^2}]|y - \widehat{y}|\\
&+ [b_3 + (a_{31} + 2a_{33} + a_{13} + a_{23} + a_{32})M)]|z - \widehat{z}|\\
&\leqslant \ell \|F(X) - F(\widehat{X})\|.
\end{aligned}$$

where

$$\begin{aligned}
\ell = \max\Big\{ & b_1 + (a_{31} + 2a_{11} + a_{13})M + \frac{(a_{21}+a_{12})(M\alpha + M^2)}{\alpha^2},\\
& b_2 + (a_{32} + 2a_{22} + a_{23})M + \frac{(a_{21}+a_{12})(M\alpha + M^2)}{\alpha^2},\\
& b_3 + (a_{31} + 2a_{33} + a_{13} + a_{23} + a_{32})M \Big\}.
\end{aligned}$$

Thus, F satisfies the local Lipschitz condition, thereby implying that the theorem holds. □

Next, we present the boundedness and non-negativity of the solutions for system (1).

Theorem 4 *All solutions of system (1) are uniformly bounded within the domain ζ, which is defined as:*

$$\zeta = \left\{(x,y,z) \in \mathbb{R}^3_+ \middle| 0 < x + y + z \leqslant \frac{b_4^2}{4a_{11}K} + \varepsilon,\ \varepsilon > 0\right\}.$$

Proof: Let us define the function:

$$\mathfrak{R}(t) = x(t) + y(t) + z(t). \tag{2}$$

Applying the Caputo fractional derivative to the above defined function (2), we obtain:

$$\begin{aligned}
&{}^cD^q\mathfrak{R}(t) = {}^cD^q x(t) + {}^cD^q y(t) + {}^cD^q z(t)\\
&= x(t)\left[b_1 - a_{11}x(t) - \frac{a_{12}y(t)}{\alpha + x(t-\tau)} - a_{13}z(t)\right]\\
&\quad + y(t)\left[-b_2 + \frac{a_{21}x(t-\tau)}{\alpha + x(t-\tau)} - a_{22}y(t) - a_{23}z(t)\right]\\
&\quad + z(t)[-b_3 + a_{31}x(t) - a_{32}y(t) - a_{33}z(t)]\\
&\leqslant b_1x(t) - a_{11}x^2(t) - b_2y(t) - a_{22}y^2(t) - b_3z(t) - a_{33}z^2(t).
\end{aligned}$$

If $\Lambda = \min\{b_2, b_3\}$, $b_4 = b_1 + \Lambda$, then the following formula is valid:

$$\begin{aligned}
{}^cD^q\mathfrak{R}(t) + \Lambda\mathfrak{R}(t) &\leqslant b_4x(t) - a_{11}x^2(t)\\
&= -a_{11}\left[x(t) - \tfrac{b_4}{2a_{11}}\right]^2 + \tfrac{b_4^2}{4a_{11}} \leqslant \tfrac{b_4^2}{4a_{11}}.
\end{aligned} \tag{3}$$

Applying the Laplace transform to Eq. (3), and denoting $F(s) = \mathscr{L}\{\Re(t)\}$, we derive the following inequality:

$$s^q F(s) - s^{q-1}\Re(0) + KF(s) \leqslant \frac{b_4^2}{4a_{11}s}.$$

From the above inequality, we can deduce that

$$F(s) \leqslant \Re(0)\frac{s^{q-1}}{s^q + K} + \frac{b_4^2}{4a_{11}s(s^q + K)}.$$

By taking the inverse Laplace transform of both sides of the above inequality, we obtain

$$\Re(t) \leqslant \Re(0)\mathscr{L}^{-1}\left\{\frac{s^{q-1}}{s^q + K}\right\} + \frac{b_4^2}{4a_{11}}\mathscr{L}^{-1}\left\{\frac{s^{q-(q+1)}}{s^q + K}\right\}.$$

Leveraging Theorem 1, we arrive at

$$\Re(t) \leqslant \Re(0)E_{q,1}\{-Kt^q\} + \frac{b_4^2}{4a_{11}}t^q E_{q,q+1}\{-Kt^q\}.$$

According to the properties of the Mittag-Leffler function, we have

$$E_{q,1}\{-Kt^q\} = (-Kt^q)E_{q,q+1}\{-Kt^q\} + \frac{1}{\Gamma(1)}.$$

Equivalently,

$$t^q E_{q,q+1}\{-Kt^q\} = -\frac{1}{K}\left[E_{q,1}\{-Kt^q\} - 1\right].$$

Consequently,

$$\Re(t) \leqslant \left\{\Re(0) - \frac{b_4^2}{4a_{11}K}\right\}E_{q,1}\{-Kt^q\} + \frac{b_4^2}{4a_{11}K}.$$

Given that $E_{q,1} \to 0$ as $t \to \infty$, all solutions of system (1) are uniformly bounded within the region

$$\zeta = \left\{(x,y,z) \in \mathbb{R}_+^3 \middle| 0 < x + y + z \leqslant \frac{b_4^2}{4a_{11}K} + \varepsilon,\ \varepsilon > 0\right\}.$$

This concludes the proof. □

Theorem 5 *All solutions to system* (1) *are inherently non-negative for all time* $t \geqslant 0$.

Proof: From the first equation of system (1), we have

$$\frac{dx^q}{dt} = x\left(b_1 - a_{11}x - \frac{a_{12}y}{\alpha + x} - a_{13}z\right).$$

Again from Theorem 4, we have

$$\Re(t) = x(t) + y(t) + z(t) \leqslant \frac{b_4^2}{4a_{11}K} = k_1.$$

Then from the above equation, we have

$$\begin{aligned}\frac{dx^q}{dt} &= x\left(b_1 - a_{11}x - \frac{a_{12}y}{\alpha + x} - a_{13}z\right)\\ &\geqslant x\left[b_1 - (a_{11} + a_{12} + a_{13})k_1\right] = x\delta_1,\end{aligned}$$

where,

$$\delta_1 = b_1 - (a_{11} + a_{12} + a_{13})k_1.$$

Now, according to the standard comparison theorem for fractional-order system (1) and the positivity of the Mittag-Leffler function $E_{\alpha,1}(t) > 0$ for any $q \in (0,1)$ [39], we have

$$x(t) \geqslant x(0)E_{\alpha,1}(\delta_1 t^q) \implies x(t) \geqslant 0.$$

Using a similar technique, we can establish that $y \geqslant 0$ and $z \geqslant 0$. Consequently, all solutions to system (1) are non-negative. □

STABILITY OF EQUILIBRIUM POINTS

In this section, we investigate the existence and local asymptotic stability of equilibrium points for system (1). The equilibrium points are characterized as follows:

Theorem 6 *The trivial equilibrium point* $E_0 = (0,0,0)$ *does not exhibit local asymptotic stability.*

Proof: The Jacobian matrix of system (1) evaluated at the trivial equilibrium point E_0 is given by:

$$J_0 = \begin{bmatrix} b_1 & 0 & 0 \\ 0 & -b_2 & 0 \\ 0 & 0 & -b_3 \end{bmatrix} \tag{4}$$

with characteristic equation

$$(\lambda - b_1)(\lambda + b_2)(\lambda + b_3) = 0,$$

and the eigenvalues of (4) are

$$\lambda_1 = b_1, \quad \lambda_2 = -b_2, \quad \lambda_3 = -b_3.$$

It is straightforward to demonstrate that

$$|\arg(\lambda_1)| = 0 < \frac{\pi q}{2}, \quad \left|\arg\left(\lambda_{2,3}\right)\right| = \pi > \frac{\pi q}{2}.$$

Thus, the trivial equilibrium point E_0 fails to exhibit local asymptotic stability. The proof is complete. □

Theorem 7 *The coexisting equilibrium point* $E_* = (x^*, y^*, z^*)$ *exhibits local asymptotic stability under the satisfaction of Hypotheses 1–5:*

Hypothesis 1. $M > 0$.

Hypothesis 2. $a_{12}Q - \alpha N < 0$.

Hypothesis 3.

$$Q+\frac{a_{23}a_{33}x^*}{a_{22}a_{33}-a_{23}a_{32}}\left(\frac{a_{21}}{a_{23}(\alpha+x^*)}-\frac{a_{31}}{a_{33}}\right)>0.$$

Hypothesis 4.

$$\frac{b_3a_{22}-b_2a_{32}}{a_{23}a_{32}-a_{22}a_{33}}+\frac{a_{22}a_{32}x^*}{a_{23}a_{32}-a_{22}a_{33}}\left(\frac{a_{21}}{a_{22}(\alpha+x^*)}-\frac{a_{31}}{a_{32}}\right)>0.$$

Hypothesis 5. $B_1>0$, $B_2>0$, $B_3>0$, $\Delta_1>0$, *where*

$$\Delta_1=\begin{bmatrix} B_1 & 1\\ B_3 & B_2\end{bmatrix}, \Delta_2=B_3\Delta_1.$$

Proof: By solving system (1), it can be shown that x^* satisfies the following relation:

$$\begin{aligned}&Mx^{*3}+(P+2\alpha M-N)x^{*2}\\&+\big(D+\alpha^2M-2\alpha N+\alpha P+a_{12}Q\big)x^*+a_{12}\alpha Q-\alpha^2N=0,\end{aligned}$$

where

$$\begin{aligned}&M=a_{11}-\tfrac{a_{13}a_{22}a_{31}}{a_{23}a_{32}-a_{22}a_{33}},\quad N=b_1-a_{13}\tfrac{b_3a_{22}-b_2a_{32}}{a_{23}a_{32}-a_{22}a_{33}},\\&P=a_{13}a_{21}-a_{12}a_{31},\ Q=\tfrac{b_3a_{23}-b_2a_{33}}{a_{22}a_{33}-a_{23}a_{32}},\ D=\tfrac{a_{12}a_{21}a_{33}}{a_{22}a_{33}-a_{23}a_{32}}.\end{aligned}$$

We now formulate an equation involving x^*:

$$\begin{aligned}f(x^*)&=Mx^{*3}+(P+2\alpha M-N)x^{*2}\\&+\big(D+\alpha^2M-2\alpha N+\alpha P+a_{12}Q\big)x^*+a_{12}\alpha Q-\alpha^2N.\end{aligned}$$

Under the satisfaction of Hypotheses 1–4, we have $\lim\limits_{x\to\infty}f(x^*)>0$ and $f(0)=a_{12}\alpha Q-\alpha^2N<0$. By the intermediate value theorem, there exists a positive solution $x^*>0$. Consequently, the coexisting equilibrium point $E_*=(x^*,y^*,z^*)$ exists, where

$$\begin{aligned}&y^*=Q+\frac{a_{23}a_{33}x^*}{a_{22}a_{33}-a_{23}a_{32}}\left(\frac{a_{21}}{a_{23}(\alpha+x^*)}-\frac{a_{31}}{a_{33}}\right),\\&z^*=\frac{b_3a_{22}-b_2a_{32}}{a_{23}a_{32}-a_{22}a_{33}}+\frac{a_{22}a_{32}x^*}{a_{23}a_{32}-a_{22}a_{33}}\left(\frac{a_{21}}{a_{22}(\alpha+x^*)}-\frac{a_{31}}{a_{32}}\right).\end{aligned}$$

The Jacobian matrix of system (1) evaluated at the coexisting equilibrium point E_* is presented as follows:

$$J_{E^*}=\begin{bmatrix}k_{11}&k_{12}&k_{13}\\k_{21}&k_{22}&k_{23}\\k_{31}&k_{32}&k_{33}\end{bmatrix},$$

where

$$\begin{aligned}&k_{11}=b_1-2a_{11}x^*-\tfrac{a_{12}(\alpha+x^*)y^*-a_{12}x^*y^*}{(\alpha+x^*)^2}-a_{13}z^*,\\&k_{12}=-\tfrac{a_{12}x^*}{(\alpha+x^*)},\ k_{13}=-a_{13}x^*,\ k_{21}=\tfrac{a_{21}(\alpha+x^*)y^*-a_{21}x^*y^*}{(\alpha+x^*)^2},\\&k_{22}=-b_2-2a_{22}y^*+\tfrac{a_{21}y^*}{(\alpha+x^*)}-a_{23}z^*,\\&k_{23}=-a_{23}y^*,\ k_{31}=a_{31}z^*,\ k_{32}=a_{32}z^*,\\&k_{33}=-b_3+a_{31}x^*-a_{32}y^*-2a_{33}z^*.\end{aligned}$$

Consequently, we get the characteristic equation, and it takes the following form:

$$\lambda^3+B_1\lambda^2+B_2\lambda+B_3=0, \tag{5}$$

where

$$\begin{aligned}&B_1=-k_{11}-k_{22}-k_{33},\\&B_2=k_{11}k_{22}+k_{22}k_{33}+k_{11}k_{33}-k_{12}k_{21}-k_{13}k_{31},\\&B_3=-k_{11}k_{22}k_{33}+k_{12}k_{21}k_{33}-k_{12}k_{23}k_{31}\\&\quad-k_{13}k_{21}k_{32}+k_{13}k_{22}k_{31}.\end{aligned}$$

Finally, by applying Hypothesis 5 and the Routh-Hurwitz criterion, we demonstrate that all eigenvalues of the characteristic Eq. (5) have negative real parts. Thus, the coexisting equilibrium point E_* exhibits local asymptotic stability when $\tau=0$. The proof is complete. □

HOPF BIFURCATION

To facilitate analytical tractability, we introduce the following transformation:

$$x=u+x^*,\quad y=v+y^*,\quad z=w+z^*.$$

System (1) is then transformed into:

$$\begin{aligned}{}^cD^qx(t)&=(u(t)+x^*)\Big[b_1-a_{11}(u(t)+x^*)\\&\quad-\frac{a_{12}(v(t)+y^*)}{\alpha+u(t-\tau)+x^*}-a_{13}(w(t)+z^*)\Big],\\{}^cD^qy(t)&=(v(t)+y^*)\Big[-b_2+\frac{a_{12}(u(t-\tau)+x^*)}{\alpha+u(t-\tau)+x^*}\\&\quad-a_{22}(v(t)+y^*)-a_{23}(w(t)+z^*)\Big],\\{}^cD^qz(t)&=(w(t)+z^*)\Big[-b_3+a_{31}(u(t)+x^*)\\&\quad-a_{32}(v(t)+y^*)-a_{33}(w(t)+z^*)\Big].\end{aligned}$$

Thus, we derive the following result:

$$\begin{aligned}{}^cD^qu(t)&=h_{11}u(t)+h_{12}v(t)+h_{13}w(t)+p_{11}u(t-\tau),\\{}^cD^qv(t)&=h_{22}v(t)+h_{23}w(t)+p_{21}u(t-\tau),\\{}^cD^qw(t)&=h_{31}u(t)+h_{32}v(t)+h_{33}w(t),\end{aligned} \tag{6}$$

where

$$\begin{aligned}&h_{11}=b_1-a_{11}x^*-a_{13}z^*,\ h_{12}=-\frac{a_{12}x^*}{\alpha+x^*},\ h_{13}=-a_{13}x^*,\\&h_{22}=-b_2-2a_{22}y^*-a_{23}z^*,\ h_{23}=-a_{23}y^*,\ h_{31}=a_{31}z^*,\\&h_{32}=-a_{32}z^*,\ h_{33}=-b_3+a_{31}x^*-a_{32}y^*-2a_{33}z^*,\\&p_{11}=-\frac{a_{12}x^*y^*}{\alpha+x^*},\ p_{21}=\frac{a_{21}y^*}{\alpha+x^*}.\end{aligned}$$

Using the Laplace transform on Eq. (6), where $\mathscr{L}(u(t))=U(s), \mathscr{L}(v(t))=V(s), \mathscr{L}(w(t))=W(s)$, we

can get

$$\begin{aligned}
s^q U(s) - s^{q-1}u(0) &= h_{11}U(s) + h_{12}V(s) + h_{13}W(s) \\
&\quad + p_{11}\,\mathrm{e}^{-st}\Big(U(s) + \int_{-\tau}^{0} \mathrm{e}^{-st}u(t)\,\mathrm{d}t\Big), \\
s^q V(s) - s^{q-1}v(0) &= h_{22}V(s) + h_{23}W(s) \\
&\quad + p_{21}\,\mathrm{e}^{-st}\Big(U(s) + \int_{-\tau}^{0} \mathrm{e}^{-st}u(t)\,\mathrm{d}t\Big), \\
s^q W(s) - s^{q-1}w(0) &= h_{31}U(s) + h_{32}V(s) + h_{33}W(s).
\end{aligned} \tag{7}$$

The characteristic equation associated with Eq. (7) is given by:

$$|\Delta(s)| = \begin{vmatrix} s^q - h_{11} - p_{11}\,\mathrm{e}^{-st} & -h_{12} & -h_{13} \\ -p_{21}\,\mathrm{e}^{-st} & s^q - h_{22} & -h_{23} \\ -h_{31} & -h_{32} & s^q - h_{33} \end{vmatrix} = 0. \tag{8}$$

The Eq. (8) can be reformulated as follows:

$$\Gamma_1(s) + \Gamma_2(s)\,\mathrm{e}^{-st} = 0, \tag{9}$$

where

$$\begin{aligned}
\Gamma_1(s) &= s^{3q} - (h_{11} + h_{22} + h_{33})s^{2q} \\
&\quad + (h_{11}h_{22} + h_{11}h_{33} + h_{22}h_{33} - h_{13}h_{31} - h_{23}h_{32})s^q \\
&\quad + (h_{11}h_{23}h_{32} + h_{13}h_{22}h_{31} - h_{11}h_{22}h_{33} - h_{12}h_{23}h_{31}), \\
\Gamma_2(s) &= -p_{11}s^{2q} + (p_{11}h_{22} + p_{11}h_{33} - p_{21}h_{12})s^q \\
&\quad + (p_{11}h_{23}h_{32} + p_{21}h_{12}h_{33} - p_{11}h_{22}h_{33} - p_{21}h_{13}h_{32}),
\end{aligned}$$

denote as

$$\begin{aligned}
\Gamma_1(s) &= s^{3q} + m_1 s^{2q} + m_2 s^q + m_3, \\
\Gamma_2(s) &= m_4 s^{2q} + m_5 s^q + m_6.
\end{aligned}$$

Suppose the pure imaginary root of Eq. (9) is $s = \mathrm{i}\omega$ ($\omega > 0$). Substituting $s = \mathrm{i}\omega$ into Eq. (9), we derive the following by equating real and imaginary parts:

$$\begin{aligned}
&(\mathrm{i}w)^{3q} + m_1(\mathrm{i}w)^{2q} + m_2(\mathrm{i}w)^q + m_3 \\
&\qquad + \big(m_4(\mathrm{i}w)^{2q} + m_5(\mathrm{i}w)^q + m_6\big)\,\mathrm{e}^{-(\mathrm{i}\hat{\mathrm{i}})\tau} = 0.
\end{aligned}$$

This implies

$$\begin{aligned}
&w^{3q}\Big(\cos\tfrac{3q\pi}{2} + \mathrm{i}\sin\tfrac{3q\pi}{2}\Big) + m_1 w^{2q}(\cos(q\pi) + \mathrm{i}\sin(q\pi)) \\
&+ m_2 w^q\Big(\cos\tfrac{q\pi}{2} + \mathrm{i}\sin\tfrac{q\pi}{2}\Big) + m_3 + m_4(\cos(q\pi) + \mathrm{i}\sin(q\pi)) \\
&\times (\cos(w\tau) - \mathrm{i}\sin(w\tau)) + m_5\Big(\cos\tfrac{q\pi}{2} + \mathrm{i}\sin\tfrac{q\pi}{2}\Big) \\
&\times (\cos(w\tau) - \mathrm{i}\sin(w\tau)) + m_6(\cos(w\tau) - \mathrm{i}\sin(w\tau)) = 0.
\end{aligned}$$

Separating the resulting expression into real and imaginary components, we obtain:

$$\begin{aligned}
E_1\cos(w\tau) + F_1\sin(w\tau) &= -E_2, \\
F_1\cos(w\tau) - E_1\sin(w\tau) &= -F_2,
\end{aligned}$$

where

$$\begin{aligned}
E_1 &= m_4\cos(q\pi) + m_5\cos\big(\tfrac{q\pi}{2}\big) + m_6, \\
E_2 &= w^{3q}\cos\tfrac{3q\pi}{2} + m_1 w^{2q}\cos(q\pi) + m_2 w^q\cos\tfrac{q\pi}{2} + m_3, \\
F_1 &= m_4\sin(q\pi) + m_5\sin\big(\tfrac{q\pi}{2}\big), \\
F_2 &= w^{3q}\sin\tfrac{3q\pi}{2} + m_1 w^{2q}\sin(q\pi) + m_2 w^q\sin\tfrac{q\pi}{2}.
\end{aligned}$$

We obtain:

$$\begin{aligned}
\cos(w\tau) &= -\frac{E_1E_2 + F_1F_2}{{E_1}^2 + F_1^2} = g_1(w), \\
\sin(w\tau) &= \frac{E_1F_2 - E_2F_1}{{E_1}^2 + F_1^2} = g_2(w),
\end{aligned}$$

using the identity $\sin^2(w\tau) + \cos^2(w\tau) = 1$, we derive the following relationship:

$$g_1^2(w) + g_2^2(w) = 1,$$

where $g_1(w) = \cos(w\tau)$. Solving for the time delay τ from the argument of the cosine function, we obtain the family of solutions

$$\tau^{(k)} = \frac{1}{w}\left[\arccos g_1(w) + 2k\pi\right], \qquad k = 0, 1, 2, \ldots,$$

where k indexes the infinite sequence of periodic solutions arising from the periodicity of the cosine function.

To identify the critical delay threshold at which a Hopf bifurcation may occur, we define the minimal positive solution from this family as:

$$\tau_0 = \min\left\{\tau^{(k)} \mid k \in \mathbb{N}_0\right\},$$

where $\mathbb{N}_0 = \{0, 1, 2, \ldots\}$ denotes the set of non-negative integers. This value τ_0 represents the smallest delay parameter for which pure imaginary roots exist, serving as the bifurcation threshold for the emergence of oscillatory behavior in the system.

To characterize the conditions under which a Hopf bifurcation arises, we posit the following necessary Hypothesis.

Hypothesis 6. $\frac{X_1Y_1 + X_2Y_2}{Y_1^2 + Y_2^2} \neq 0$, where the expressions for X_i, Y_i ($i = 1, 2$) are defined in Eq. (10).

Theorem 8 *Let $s(\tau) = \alpha(\tau) + \mathrm{i}\eta(\tau)$ denote the root of (9) such that near the critical delay $\tau = \tau_0$, it satisfies $\alpha(\tau_0) = 0$ and $\eta(\tau_0) = \eta_0$, where $\eta_0 > 0$ is the angular frequency at the bifurcation point. Under these conditions and the satisfaction of Hypotheses 6, the transversal condition*

$$\mathrm{Re}\left[\frac{\mathrm{d}s}{\mathrm{d}\tau}\right]\Bigg|_{(\tau=\tau_0, \omega=\omega_0)} \neq 0$$

is satisfied, ensuring that the eigenvalue crosses the imaginary axis with non-zero speed as τ varies through τ_0.

Proof: To verify the transversality condition for the Hopf bifurcation, we take the derivative of both sides of the characteristic Eq. (9) with respect to the delay parameter τ. This yields

$$\Gamma_1'(s)\tfrac{\mathrm{d}s}{\mathrm{d}\tau}+\Gamma_2'(s)\tfrac{\mathrm{d}s}{\mathrm{d}\tau}\,\mathrm{e}^{-s\tau}-\tau\Gamma_2(s)\tfrac{\mathrm{d}s}{\mathrm{d}\tau}\,\mathrm{e}^{-s\tau}-s\Gamma_2(s)\,\mathrm{e}^{-s\tau}=0,$$

simplified to

$$\frac{\mathrm{d}s}{\mathrm{d}\tau}=\frac{s\Gamma_2(s)\,\mathrm{e}^{-s\tau}}{\Gamma_1'(s)+\Gamma_2{}'(s)\,\mathrm{e}^{-s\tau}-\tau\Gamma_2(s)\,\mathrm{e}^{-s\tau}}.$$

By Hypothesis 6, we obtain

$$\mathrm{Re}\left[\frac{\mathrm{d}s}{\mathrm{d}\tau}\right]=\frac{X_1Y_1+X_2Y_2}{Y_1^2+Y_2^2}\neq 0,$$

where

$$\begin{aligned}
X_1&=\mathrm{Re}\left[\Gamma_2(\mathrm{i}w_0)\,\mathrm{e}^{-\mathrm{i}w_0\tau_0}\mathrm{i}w_0\right],\\
X_2&=\mathrm{Im}\left[\Gamma_2(\mathrm{i}w_0)\,\mathrm{e}^{-\mathrm{i}w_0\tau_0}\mathrm{i}w_0\right],\\
Y_1&=\mathrm{Re}\left[\Gamma_1'(\mathrm{i}w_0)+\Gamma_2'(\mathrm{i}w_0)\,\mathrm{e}^{-\mathrm{i}w_0\tau_0}-\Gamma_2(\mathrm{i}w_0)\,\mathrm{e}^{-\mathrm{i}w_0\tau_0}\tau_0\right],\\
Y_2&=\mathrm{Im}\left[\Gamma_1'(\mathrm{i}w_0)+\Gamma_2'(\mathrm{i}w_0)\,\mathrm{e}^{-\mathrm{i}w_0\tau_0}-\Gamma_2(\mathrm{i}w_0)\,\mathrm{e}^{-\mathrm{i}w_0\tau_0}\tau_0\right].
\end{aligned}\tag{10}$$

□

Based on Hypotheses 1–6, the following results can be established for system (1).

Corollary 1 *If Hypotheses 1–6 are all satisfied, the following conclusions can be drawn:*

(i) If $\tau\in[0,\tau_0)$, then the E_* of system (1) is asymptotically stable.

(ii) The E_* of system (1) is unstable when $\tau>\tau_0$.

(iii) If $\tau=\tau_0$, then system (1) undergoes a Hopf bifurcation.

NUMERICAL SIMULATIONS

In this section, numerical simulations are conducted to validate the theoretical results derived in preceding sections. Additionally, the influence of the fractional order on the bifurcation onset is systematically explored. Consider the following parameter values:

$$\begin{aligned}
&\alpha=0.5,\ b_1=2,\ b_2=0.32,\ b_3=0.4,\ a_{11}=0.9,\\
&a_{12}=0.75,\ a_{13}=0.5,\ a_{21}=1.375,\ a_{22}=0.2,\\
&a_{23}=0.3,\ a_{31}=0.24,a_{32}=0.35,a_{33}=0.3.
\end{aligned}\tag{11}$$

Direct computations confirm that Hypotheses 1–5 are satisfied, and the existence of the coexisting equilibrium point $E^*=(x^*,y^*,z^*)=(0.653,2.134,0.234)$ is rigorously established. The initial conditions are set as $(x(0),y(0),z(0))=(2.00,3.00,2.00)$. We now investigate the effects of key system parameters on the dynamical behavior of the system.

Case 1: The influence of fractional orders on the stability region is analyzed.

We set $\tau=0$ and initially examine the impact of the fractional order on the convergence rate of the solution towards the equilibrium point. Fig. 1 depicts the oscillatory characteristics of the solutions within the fractional-order system for various fractional orders.

Fig. 1 demonstrates that the oscillatory characteristics of the solution become more pronounced as the fractional order increases. When the order increases from 0.85 to 0.95, the amplitude and frequency of oscillations intensify significantly, thereby illustrating the critical role of the fractional order in modulating the stability region of the system.

Fig. 2 illustrates the local asymptotic stability of the system's equilibrium point across different fractional orders. Where Figure 2(a) and (b) for the orders $q=0.85$; Fig. 2(c,d) for the orders $q=0.90$, Fig. 2(e,f) for the orders $q=0.95$, Fig. 2(g,h) for the orders $q=0.99$.

Remark 1 When $q=1.00$, the fractional-order system reduces to an integer-order system. Given that the fractional-order system exhibits instability at $q=0.99$, the integer-order counterpart is necessarily unstable in this scenario. This observation highlights that the stability region of the fractional-order system is significantly broader than that of its integer-order counterpart. From a biological perspective, this phenomenon can be interpreted as follows: the population dynamics incorporate a "memory effect", where historical behavioral patterns (analogous to the fractional-order system's past-state dependence) influence current interactions. This memory characteristic-intrinsic to fractional-order modeling-reflects how animals leverage cumulative past experiences to modulate present behavior, which in turn provides a evolutionary advantage by promoting long-term species stability and adaptability.

Case 2: The influence of time delays on system stability and the occurrence of Hopf bifurcation is analyzed.

In this section, we employ the time delay τ as the bifurcation parameter to investigate the stability of the equilibrium point E^* and the occurrence of Hopf bifurcation with respect to τ. Setting the fractional order $q=0.90$, we derive the critical bifurcation point $\tau_0=2.956$ through analytical calculations. This result confirms that system (1) undergoes a Hopf bifurcation at the equilibrium E^* when the delay parameter reaches $\tau_0=2.956$, as demonstrated in Fig. 3.

From Remark 1, it follows that E^* is locally asymptotically stable when the delay parameter $\tau=2.85$ is less than the critical value τ_0. This stability is visualized in Fig. 4(a,b), which display the time-series plots and phase portraits, respectively. Conversely, when $\tau=3.00$ exceeds τ_0, E^* loses stability, as illustrated in Fig. 4(c,d), where the corresponding time-series and phase diagrams exhibit divergent behavior. Fig. 5 illustrates the influence of the fractional order sequence q on the bifurcation point τ_0.

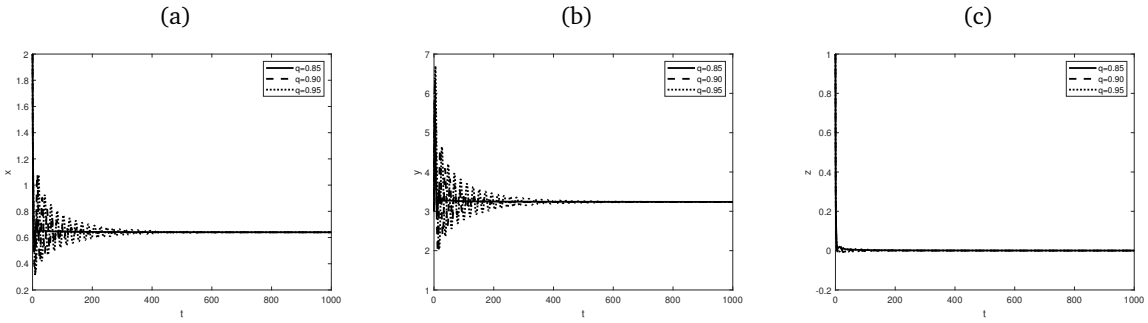

Fig. 1 Local asymptotic stability diagram of system at E^* when $q = 0.85, 0.90, 0.95$. (a) Stability of x when $q = 0.85, 0.90, 0.95$. (b) Stability of y when $q = 0.85, 0.90, 0.95$. (c) Stability of z when $q = 0.85, 0.90, 0.95$.

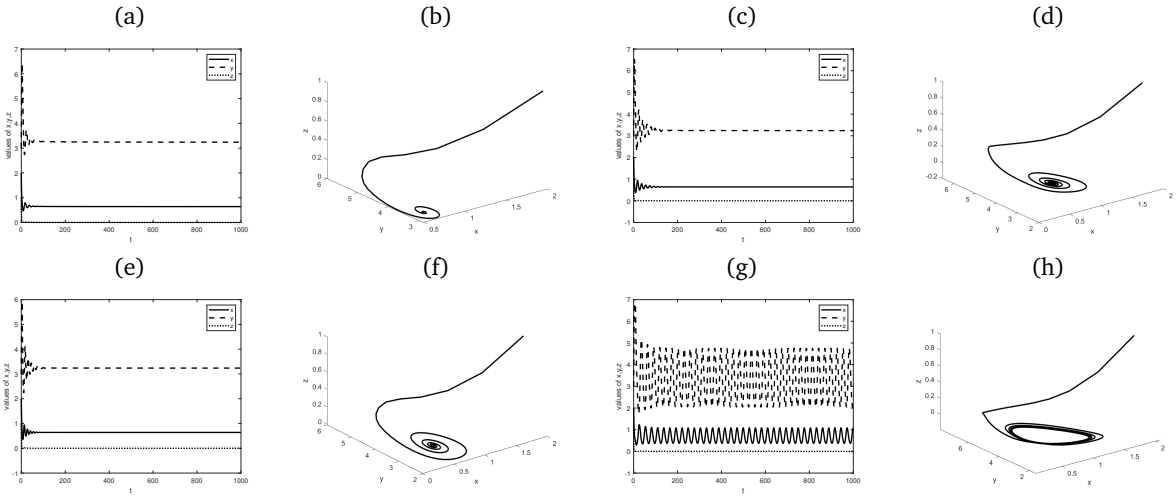

Fig. 2 Dynamical behavior of system (1) under different q. (a, b) The time series and phase diagram when q= 0.85; (c d) the time series and phase diagram when $q = 0.90$; (e, f) the time series and phase diagram when $q = 0.95$; and (g,h) the time series and phase diagram when $q = 0.99$.

CONCLUSION

This study presents a comprehensive analysis of a fractional-order delayed predator-prey system with ratio dependence, incorporating a Holling-II functional response to model nonlinear trophic interactions. By leveraging the Caputo fractional derivative, the system captures memory effects and hereditary traits inherent in ecological dynamics, offering a more realistic representation of population behaviors compared to classical integer-order models. The boundedness and existence of solutions were rigorously established using Laplace transform techniques and fixed-point theorems, ensuring the model's mathematical well-

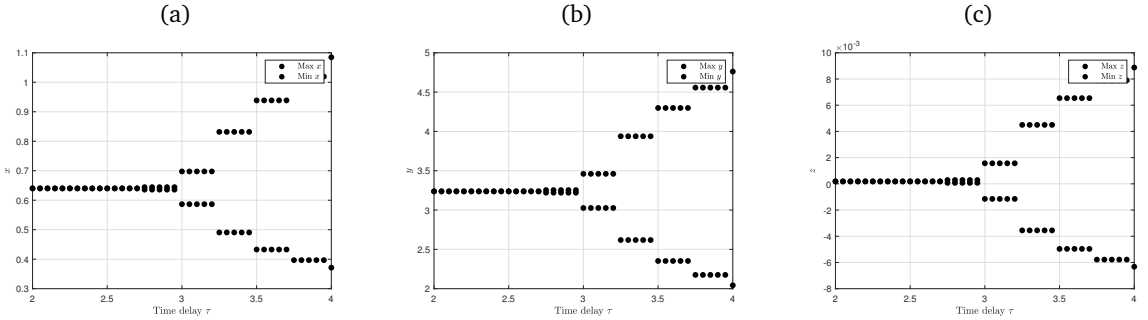

Fig. 3 Hopf bifurcation phase diagrams of the system (1) when $q = 0.90$. The Hopf bifurcation point is $\tau_0 = 2.956$.

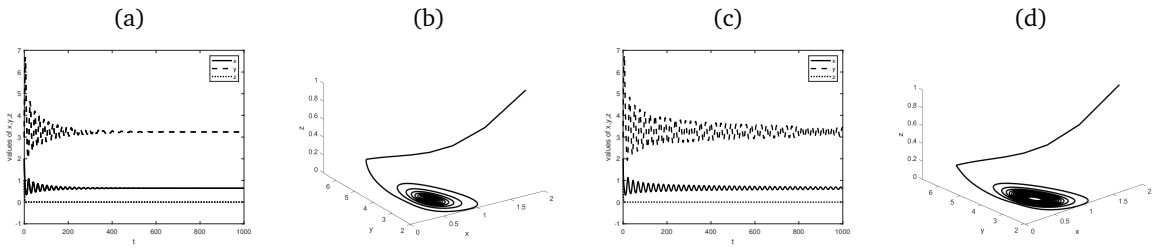

Fig. 4 (a, b) The time series and phase diagram when $q = 0.90$, $\tau = 2.85 < \tau_0$; (c, d) the time series and phase diagram when $q = 0.90$, $\tau = 3.00 > \tau_0$.

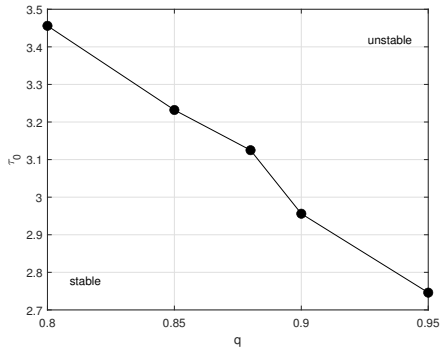

Fig. 5 The effect of fractional order sequence q on bifurcation point τ_0.

posedness. Furthermore, stability analysis of equilibrium points revealed that the system's dynamics are highly sensitive to both fractional orders and time delays, with critical thresholds identified for stability transitions. These theoretical advancements provide a robust framework for understanding complex predator-prey interactions, particularly in systems where historical dependencies and delayed feedback play pivotal roles.

Numerical simulations were employed to validate the analytical results, demonstrating that higher fractional orders amplify oscillatory behavior, while time delays induce Hopf bifurcations, leading to periodic solutions. For instance, at a fractional order of $q = 0.90$, the system exhibited a bifurcation at a critical delay of $\tau_0 = 2.956$, transitioning from stable equilibrium to sustained oscillations. These findings underscore the importance of fractional calculus in ecological modeling, as it accounts for memory effects that influence population dynamics over time. The simulations also highlighted the broader stability regions of fractional-order systems compared to their integer-order counterparts, suggesting that fractional models are better suited for capturing the long-term adaptive behaviors observed in natural ecosystems.

The study's insights have significant implications for ecological theory and conservation strategies, particularly in systems like the Arctic tundra, where predator-prey interactions are influenced by delayed responses and environmental memory. Future research could extend this framework to the control of Hopf bifurcation in fractional-order predator-prey models or to interactions among multiple species, so as to further enhance its applicability. Additionally, exploring the role of fractional orders in other biological systems, such as disease dynamics or resource competition, could yield novel insights. By bridging mathematical rigor with ecological relevance, this work contributes to a deeper understanding of the intricate balance governing predator-prey dynamics and opens new avenues for interdisciplinary exploration in mathematical biology.

Acknowledgements: This research is supported by the National Natural Science Foundation of Xinjiang Uygur Autonomous Region (grant no. 2025D01C41) and the Open Project of Xinjiang Key Laboratory of Applied Mathematics(grant no. 2023D04045).

REFERENCES

1. Lotka AJ (1925) *Elements of Physical Biology*, 1st edn, Williams & Wilkins, Baltimore.
2. Lotka AJ (1927) Fluctuations in the abundance of a species considered mathematically. *Nature* **119**, 12.
3. Yüzbaşı Ş (2021) An operational matrix method to solve the Lotka-Volterra predator-prey models with discrete delays. *Chaos Solitons Fractals* **153**, 111482.
4. Ma Z, Chen F, Wu C (2013) Dynamic behaviors of a Lotka-Volterra predator-prey model incorporating a prey refuge and predator mutual interference. *Appl Math Comput* **219**, 7945–7953.
5. Ma ZP, Yue JL (2016) Competitive exclusion and coexistence of a delayed reaction-diffusion system modeling two predators competing for one prey. *Appl Math Comput* **71**, 1799–1817.
6. Bi Z, Liu S, Ouyang M (2022) Three-dimensional pattern dynamics of a fractional predator-prey model with cross-diffusion and herd behavior. *Appl Math Comput* **421**, 126955.
7. Das D, Bhattacharjee D (2025) An investigation into the impact of odour: A dynamical study of two predators and one prey model, taking into account both integer order and fractional order derivatives. *Math Comput Simul* **233**, 341–368.
8. Wu S, Wang Y, Geng D (2025) Dynamic and pattern formation of a diffusive predator-prey model with in-

direct prey-taxis and indirect predator-taxis. *Nonlinear Anal Real World Appl* **84**, 104299.
9. Zhang H, Muhammadhaji A (2024) Dynamics of a delayed fractional-order predator-prey model with cannibalism and disease in prey. *Fractal Fract* **8**, 333.
10. Du W, Xiao M, Ding J, Yao Y, Wang Z, Yang X (2023) Fractional-order PD control at Hopf bifurcation in a delayed predator-prey system with trans-species infectious diseases. *Math Comput Simul* **205**, 414–438.
11. Mao S, Zhang Y, Kang Y, Mao Y (2021) Coopetition analysis in industry upgrade and urban expansion based on fractional derivative gray Lotka-Volterra model. *Soft Comput* **25**, 11485–11507.
12. Wang ZX, Li YT, Gao LF (2024) Identification of the dynamic trade relationship between China and the United States using the quantile grey Lotka-Volterra model. *Fractal Fract* **8**, 171.
13. Babbs CF (2012) Predicting success or failure of immunotherapy for cancer: insights from a clinically applicable mathematical model. *Am J Cancer Res* **2**, 204–213.
14. Li M, Xie N, Zhang R, Huang X (2022) Dynamics of a discrete Lotka-Volterra information diffusion model. *Int J Bifurcation Chaos* **32**, 2250228.
15. Zhang Y, Tang C, Weigang L (2014) Cooperative and competitive dynamics model for information propagation in online social networks. *J Appl Math* **2014**, 610382.
16. Kumar A, Kumar S, Momani S, Hadid S (2024) A chaos study of fractal-fractional predator-prey model of mathematical ecology. *Math Comput Simul* **225**, 857–888.
17. Rihan FA, Rajivganthi C (2020) Dynamics of fractional-order delay differential model of prey-predator system with Holling-type III and infection among predators. *Chaos Solitons Fractals* **141**, 110365.
18. Wang B, Li X (2023) Modeling and dynamical analysis of a fractional-order predator-prey system with anti-predator behavior and a Holling type IV functional response. *Fractal Fract* **7**, 722.
19. Sun XK, Huo HF, Ma CC (2013) Hopf bifurcation and stability in predator-prey model with a stage-structure for prey. *Appl Math Comput* **219**, 10313–10324.
20. Guo G, Li B (2012) The uniqueness of positive solutions for a predator-prey model with B-D functional response. In: Jin D, Lin S (eds) *Advances in Future Computer and Control Systems. Advances in Intelligent and Soft Computing*, vol 160, Springer, Berlin, Heidelberg. pp 263–269.
21. Maji C (2022) Dynamical analysis of a fractional-order predator-prey model incorporating a constant prey refuge and nonlinear incident rate. *Model Earth Syst Environ* **8**, 47–57.
22. Xie B, Zhang Z (2023) Impact of Allee and fear effects in a fractional order prey-predator system incorporating prey refuge. *Chaos* **33**, 013131.
23. Mandal M, Jana S, Nandi SK (2021) Modeling and analysis of a fractional-order prey-predator system incorporating harvesting. *Model Earth Syst Environ* **7**, 1159–1176.
24. Song P, Zhao H, Zhang X (2016) Dynamic analysis of a fractional order delayed predator-prey system with harvesting. *Theory Biosci* **135**, 59–72.
25. Kumar D, Singh J, Baleanu D (2024) Dynamical and computational analysis of a fractional predator-prey model with an infectious disease and harvesting policy. *AIMS Math* **9**, 36082–36101.
26. Singh J, Ghanbari B, Dubey VP, Kumar D, Nisar K (2024) Fractional dynamics and computational analysis of food chain model with disease in intermediate predator. *AIMS Math* **9**, 17089–17121.
27. Kumar GR, Ramesh K, Khan A, Lakshminarayan K, Abdeljawad T (2024) Bazykin predator-prey model includes a dynamical analysis of a Caputo fractional order delay fear and the effect of the population-based mortality rate on the growth of predators. *Qual Theory Dyn Syst* **23**, 130.
28. Lv X, Lu S, Yan P (2010) Existence and global attractivity of positive periodic solutions of Lotka-Volterra predator-prey systems with deviating arguments. *Nonlinear Anal Real World Appl* **11**, 574–583.
29. Zhang H, Muhammadhaji A (2024) A delayed fractional-order predator-prey model with three-stage structure and cannibalism for prey. *Fractal Fract* **8**, 492.
30. Li P, Gao R, Xu C, Li Y, Akgül A, Baleanu D (2023) Dynamics exploration for a fractional-order delayed zooplankton-phytoplankton system. *Chaos Solitons Fractals* **166**, 112975.
31. Du X, Qiu J, Lu Y, Cao J (2025) Stability and dynamics analysis of time-delay fractional-order large-scale dual-loop neural network model with cross-coupling structure. *IEEE Trans Neural Netw Learn Syst* **36**, 7873–7887.
32. Wang H, Xiao M, Tao B, Xu F, Wang Z, Huang C, Qiu J (2020) Improving dynamics of integer-order small-world network models under fractional-order PD control. *Sci China Inf Sci* **63**, 112206.
33. Xu C, Farman M, Pang Y, Liu Z, Liao M, Yao L, Shehzad A, Amilo D (2025) Mathematical analysis and dynamical transmission of (SEI_rI_sR) model with different infection stages by using fractional operator. *Int J Biomath* **2025**, 2450151.
34. Xing R, Xiao M, Zhang Y, Qiu J (2022) Stability and Hopf bifurcation analysis of an $(n+m)$-neuron double-ring neural network model with multiple time delays. *J Syst Sci Complex* **35**, 159–178.
35. Xu C, Liao M, Farman M, Shehzade A (2024) Hydrogenolysis of glycerol by heterogeneous catalysis: A fractional order kinetic model with analysis. *MATCH Commun Math Comput Chem* **91**, 635–664.
36. Zhao Y, Xu C, Xu Y, Lin J, Pang Y, Liu Z, Shen J (2024) Mathematical exploration on control of bifurcation for a 3D predator-prey model with delay. *AIMS Math* **9**, 29883–29915.
37. Lin J, Xu C, Xu Y, Zhao Y, Pang Y, Liu Z, Shen J (2024) Bifurcation and controller design in a 3D delayed predator-prey model. *AIMS Math* **9**, 33891–33929.
38. Lin J, Xu C, Zhao Y, Deng Q (2025) Hopf bifurcation and controller design for a predator-prey model with double delays. *AIP Adv* **15**, 075329.
39. Prabir P (2019) Dynamics of a fractional order predator-prey model with intraguild predation.*Int J Model Simul* **39**, 256–268.